Proceedings of the 3rd International Symposium on Uncertainty Quantification and Stochastic Modeling
D.A. Rade; A. M. G. Lima (Editors), ABCM, Maresias, SP, Brazil, February 15-19, 2016

Stochastic modeling of uncertainties in the piezoelectric coupling coefficient in arbitrary shell structures

Scinocca, F. [1] and Nabarrete, A. [1]

[1] Instituto Tecnológico de Aeronáutica - ITA, São José dos Campos, 12228-900, SP, Brazil

Abstract: *The analysis of uncertainties is extremely convenient during the project conception phase of vibration control systems, supporting scientists and engineers to obtain effectiveness in the vibration attenuation. For that, the present paper proposes a systematic approach to quantify the uncertainties when piezoelectric transducers are applied in arbitrary thin shell structures with asymmetric double curvature. These types of structures are of interest in the automotive or aeronautical applications. The variability in the optimal piezoelectric electromechanical coupling coefficient and in the dynamic behavior of the mechanical structure were studied in details. The randomness effects arising from the manufacturing process, such as stamping spring back effects, as well as in the boundary conditions, were taken into account in the analysis. Likewise, the effects of variability during the PZT patch positioning. Sensitivity and spectral analysis were employed to study the impact of randomness in the optimal piezoelectric implementation in real applications.*

Keywords: Uncertainty Quantification Analysis, Stochastic Finite Element Method, Monte Carlo Simulation, Piezoelectric Optimization, Stochastic Model Updating.

INTRODUCTION

A significant improvement in the products quality was observed in the last decades. Counting with virtual analysis, products with high level of sophistication associated with optimal performance and reliability are obtained. For engineering requirements, the Finite Element Method (FEM) deserve a prominent position among the computational tools. The FEM supports engineers and scientists to obtain optimal products in a short time schedule, due to its good predictability (Vanderplaatz, 2005). However, discrepancies between experimental and virtual results are found and need to be investigated (Scinocca, 2012). The investigation suggest that the major cause of discrepancies between virtual and experimental results are linked to the inherent randomness of the system, introducing uncertainties in the product performance results (Markowitz and Tadeusz, 2012). Randomness can be found in several important input parameters defined in FE (Finite Element) models, such as material properties, dimensions, temperature, etc. Therewith, becomes clear that just a deterministic approach is not enough to express all possible results obtained in real products performance. Aiming to analyze theses discrepancies a probabilistic approach should be adopted (Ghanem and Spanos, 2003; Soize, 2013). Therefore, using a probabilistic approach more predictable models can be obtained, helping to understand and quantify the uncertainties present in the system. For this purpose, the stochastic finite element method (SFEM) was developed. The SFEM incorporates the randomness in the analysis using a very sophisticated statistical theory grounded it. Computing the inherent randomness, the SFEM deals with the models uncertainties in a systematic way (Stefanou, 2009).

Now with the design approach able to incorporate and quantify the uncertainties during the virtual analysis phase, significant improvements in quality, reliability and performance can be obtained. Counting with the advantage of have virtual results during the product development phase, several preliminary analysis can be addressed. These preliminary analyses, such as sensitivity analysis of relevant parameter randomness in the product performance, are able to support scientists and engineers. In this way, products which present low sensitivity to randomness can be obtained, In special, the automotive industry suffers increasing pressure to maximize the energy efficiency in a sustainable way for new conceptual or reuse vehicles and materials (McKenna, R.; et.al, 2013). In a different way from traditional structural vehicle design, which takes in account the mass raising for diminishing the riding vibration, modern and optimized automotive structures use Arbitrary Thin Shell Structures(ATSS) that are excellent to obtain optimized aerodynamic performance associated with mass reduction, maximizing the vehicular weight/power ratio (Cirak, et.al, 2002; Zhang, Zhu and Chen, 2007).

For these new automotive structures or even for structural redesign for electrical vehicles, the new dynamical characteristics should be studied in details. Later with the well-known dynamic characteristics of the mechanical structure, the usage of piezoelectric absolvers could be advantageous, to control unwanted vibration levels. Similarly, electronic devices present a significant decrement in their life cycle when subjected to high vibration levels. In this way, vibration control using piezoelectric absolvers should also be considered to solve this issue for typical applications in aircrafts and automotive vehicles. Due to the low cost of implementation when compared with active vibration control techniques, the employability needs to be analyzed in large-scale production, as well as for typical Arbitrary Thin Shell Structures (ATSS) of interest, normally found in automotive or aeronautical applications. Thus, to ensure the effectiveness of these techniques, the uncertainties arising from the manufacture process randomness must be take into account in the analysis.

Therefore, the present paper aims to contribute with the uncertainty quantification of optimal piezoelectric implementation in ATSS. An analysis of the effects of the randomness in the optimal piezoelectric electromechanical coupling coefficient (EMCC) was performed. This analysis took into account the effects of the randomness arising from the manufacturing process of the mechanical structure, such as stamping spring back effects, as well as the variability in the boundary conditions of the mechanical structure. Likewise, the analysis study the effect of the variability of the PZT positioning in the structure surface, during its application process. Sensitivity and spectral analysis were performed in order to obtain a better understanding of the uncertainties effects. The main objective of this paper is to provide guidelines to maximize the effectiveness of the piezoelectric implementation for smart structures in real ATSS with complex shape design of interest in automotive and aeronautical applications.

MODELING OF UNCERTAINTIES IN PIEZOELECTRIC APPLICATIONS

The Finite Element Method (FEM) is a convenient way to modeling piezoelectric patches in complex structures, such as ATSS; however, a stochastic approach needs to be intended to introduce the randomness in FE models. For that, the Stochastic Finite Element Method (SFEM) is the appropriated way. The SFEM uses random fields to incorporate uncertainties in the model parameters, such as shell width and length, thickness, curvature, piezoelectric capacitance, dielectric properties, etc. Introducing a set of random fields, named by $b_X = (b_1, b_{2,} \dots b_n)$, that represents the randomness in the model parameters, the equation of motion for the structural assembly, ATSS and piezoelectric patches, including uncertainties becomes (Scinocca, 2012; Soize, 2013; Neubauer and Wallaschek, 2013).

$$\begin{bmatrix} \mathbf{M}_{mm}(b_X) & \mathbf{0} \\ \mathbf{0} & \mathbf{0} \end{bmatrix} \begin{Bmatrix} \ddot{\mathbf{u}}(b_X, t) \\ \ddot{\mathbf{v}}^*(b_X, t) \end{Bmatrix} + \begin{bmatrix} \mathbf{K}_{mm}(b_X) & \mathbf{K}_{me}\,(b_X) \\ \mathbf{K}_{me}{}^T(b_X) & \mathbf{K}_{ee}\,(b_X) \end{bmatrix} \begin{Bmatrix} \mathbf{u}(b_X) \\ \mathbf{v}^*(b_X) \end{Bmatrix} = \begin{Bmatrix} \mathbf{f}(t) \\ \mathbf{q}^*(t) \end{Bmatrix} \tag{1}$$

In equation (1), $\mathbf{u}(b_X)$ and $\mathbf{v}^*(b_X)$ are partitioned random vectors representing displacement and voltage degrees of freedom. In details, $\mathbf{f}(t)$ is the vector of applied forces and $\mathbf{q}^*(t)$ represent electrical charges. $\mathbf{K}_{mm}(b_X)$ and $\mathbf{M}_{mm}(b_X)$ represent the mechanical stiffness and mass matrices of the whole mechanical structure, $\mathbf{K}_{me}\,(b_X)$ the coupling matrix between electrical and mechanical subsystems, and $\mathbf{K}_{ee}\,(b_X)$ the relation between electric charges and voltages, of the partitioned terms of the random mass and stiffness matrices.

The piezoelectric capacitance is obtained using a linear transformation such as:

$$\mathbf{v}^*(b_X) = \mathbf{G}\,\mathbf{v}\,(b_X) \tag{2}$$

The linear transformation described in equation (2) relates all electrical nodal degrees freedom, $\mathbf{v}^*(b_x)$, to the voltage of the piezoelectric patch electrode, $\mathbf{v}\,(b_x)$. By multiplying the second equation by $\mathbf{G}^T$, the equation (1) becomes:

$$\begin{bmatrix} \mathbf{M}_{mm}(b_X) & \mathbf{0} \\ \mathbf{0} & \mathbf{0} \end{bmatrix} \begin{Bmatrix} \ddot{\mathbf{u}}(b_X, t) \\ \ddot{\mathbf{v}}\,(b_X, t) \end{Bmatrix} + \begin{bmatrix} \mathbf{K}_{mm}(b_X) & \mathbf{K}_{me}\,(b_X)\,G \\ \mathbf{G}^T\,K_{me}{}^T(b_X) & -\,\mathbf{C}_p\,(b_X) \end{bmatrix} \begin{Bmatrix} \mathbf{u}(b_X) \\ \mathbf{v}\,(b_X) \end{Bmatrix} = \begin{Bmatrix} \mathbf{f}(t) \\ \mathbf{q}\,(t) \end{Bmatrix} \tag{3}$$

The piezoelectric capacitance $\mathbf{C}_p\,(b_X)$, represented in equation (3), is given by $\mathbf{C}_p\,(b_X) = -\mathbf{G}^T\mathbf{K}_{ee}\,(b_X)\,\mathbf{G}$. Consequently, $\mathbf{q}\,(t)$ is the electrode charges. Since $\mathbf{K}_{ee}\,(b_X)$ elements are negative, the piezoelectric capacitance random value becomes positive. A mass-normalized modal transformation $\mathbf{T}\,(b_X)$ is applied to the mechanical degrees of freedom in equation (3), in the form:

$$\begin{bmatrix} \mathbf{I} & \mathbf{0} \\ \mathbf{0} & \mathbf{0} \end{bmatrix} \begin{Bmatrix} \ddot{\boldsymbol{\eta}}(b_X) \\ \ddot{\mathbf{v}}\,(b_X) \end{Bmatrix} + \begin{bmatrix} \boldsymbol{\Lambda}(b_X) & \boldsymbol{\mathcal{K}}\,(b_X) \\ \boldsymbol{\mathcal{K}}^T(b_X) & -\,\mathbf{C}_p\,(b_X) \end{bmatrix} \begin{Bmatrix} \boldsymbol{\eta}(b_X) \\ \mathbf{v}\,(b_X) \end{Bmatrix} = \begin{Bmatrix} \mathbf{T}^T(b_X)\mathbf{f}(t) \\ \mathbf{q}\,(b_X) \end{Bmatrix} \tag{4}$$

In equation (4), $\mathbf{\Lambda}(b_x)$ is a diagonal matrix of squared eigenfrequencies. $\boldsymbol{\mathcal{K}}\,(b_X)$ is the coupling between the modal mechanical and electrical degrees of freedom, obtained by the static analysis of the structure. Each element $\boldsymbol{\mathcal{K}}_{ij}\,(b_X)$ represents the coupling of the *i-th* mechanical degree of freedom $\boldsymbol{\eta}_i(b_X)$ to the *j-th* voltage of the piezoelectric patch electrode. Both are evaluated as described in equation (5).

$$\mathbf{\Lambda}(b_x) = \mathbf{T}^T(b_x)\mathbf{K}_{mm}(b_x)\mathbf{T}\,(b_x) \qquad \boldsymbol{\mathcal{K}}\,(b_X) = \mathbf{T}^T(b_X)\mathbf{K}_{me}\,(b_X)\,\mathbf{G} \tag{5}$$

From equation (4), the stochastic differential equation for each *n* mechanical modal coordinates becomes:

$$\ddot{\eta}_i(b_X) + \omega_i^2(b_X)\eta_i(b_X) + \sum_{m=1}^{n} \mathcal{K}_{im}\,(b_X)\,v_m\,(b_X) = T_i^{\,T}(b_X)f_i(t) \tag{5}$$

Similarly, for the *n* electrical degree of freedom is:

$$\sum_{m=1}^{n} \mathcal{K}_{mi}\,(b_X)\,\eta_m\,(b_X) - C_{p,i}\,(b_X)v_i\,(b_X) = q_i\,(b_X) \tag{6}$$

Aiming to find the coupling of a single piezoelectric patch, the $\boldsymbol{\mathcal{K}}\,(b_X)$ matrix becomes a simple random vector, with $\mathbf{C}_p\,(b_X)$ and $\mathbf{v}\,(b_X)$ being random scalar numbers. For the special case with the electrode in short circuit the voltage is zero, and the terms $\omega_i(b_X)$ in the matrix $\mathbf{\Lambda}_{short}(b_X)$ denote the eigenfrequencies of the mechanical structure with the piezoelectric patch electrode in short circuit, such as:

$$\ddot{\boldsymbol{\eta}}\,(b_X) + \mathbf{\Lambda}_{short}(b_X)\boldsymbol{\eta}(b_X) = 0 \tag{7}$$

In equation (7), $\mathbf{\Lambda}_{short}(b_X) = diag\,(\omega_{short,i}^2(b_X))$. For the case of piezoelectric patch open electrodes the values of charge and voltage becomes $q\,(b_X) = 0$ and $v\,(b_X) = C_p^{\,-1}\,(b_X)\boldsymbol{\mathcal{K}}^T(b_X)\boldsymbol{\eta}(b_X)$ respectively, so:

$$\ddot{\boldsymbol{\eta}}\,(b_X) + \left(\mathbf{\Lambda}_{open}(b_X)\right)\boldsymbol{\eta}(b_X) = 0 \tag{8}$$

Where

$$\mathbf{\Lambda}_{open}(b_X) = \mathbf{\Lambda}_{short}(b_X) + \boldsymbol{\mathcal{K}}\,(b_X)C_p^{\,-1}\,(b_X)\boldsymbol{\mathcal{K}}^T(b_X) \tag{9}$$

The term $\boldsymbol{\mathcal{K}}\,(b_x)C_p^{\,-1}\,(b_x)\boldsymbol{\mathcal{K}}^T(b_x)$ is not a diagonal matrix. Therefore the piezoelectric patch open electrode is not a decoupled system. However, the diagonal elements are dominant in the matrix $\mathbf{\Lambda}_{open}(b_X)$, and being a good approximation for the eigenfrequencies with open electrodes. In this way resulting in:

$$diag\left(\Lambda_{open}(b_X)\right) = \omega_{open,i}^2(b_X) = \omega_{short,i}^2(b_X) + \frac{\mathcal{K}_{\,i}^{\,2}(b_X)}{C_p\,(b_X)} \tag{10}$$

The eigenfrequencies with open electrodes are higher than with piezoelectric patch short circuit or equal when the coupling $\mathcal{K}_{\,i}(b_x)$ is zero. In this way, the definition of the generalized Eletromechanical Coupling Coefficient (EMCC) is dependent of the increase in frequency of the individual eigenform and defined by:

$$\mathbb{K}_{\,i}^{\,2}(b_X) = \frac{\omega_{open,i}^2(b_X) - \omega^2_{short,i}(b_X)}{\omega_{open,i}^2(b_X)} \tag{11}$$

The EMCC identifies the piezoelectric patch capacity of transform mechanical vibration energy into electrical energy, and vice versa. For an optimal implementation of piezoelectric patches this coefficient need to be maximized taking into account the uncertainties in the analysis.

IMPLEMENTATION UNDER UNCERTAINTIES

Model updating

External structures, commonly known as outer or design structures, of interest in the automotive or aeronautical applications possess complex shapes. These complex shapes arise from virtual simulations, design studio or wind tunnel tests. Typically, these complex shapes are obtained using virtual simulations during the product conception phase. Posteriorly, physical tests are conducted in the prototype parts in order to validate the product performance. Due to uncertainties arising from the manufacturing process of the prototype parts and later from the conventional manufacturing process, discrepancies between the results obtained from FE models and physical tests are found, and model updating should be intended. In a rational manner, the best parameters to be considered in the model updating are those susceptible to uncertainties, which posteriorly can be employed in the stochastic approach to incorporate the randomness in the SFEM model (Maresa; Mottershead; Friswell, 2006; Mottershead, et al., 2006; Mottershead; Link and Friswell, 2011). In the present research, an ATSS with asymmetric double curvature configuration was selected according with Fig. 1.

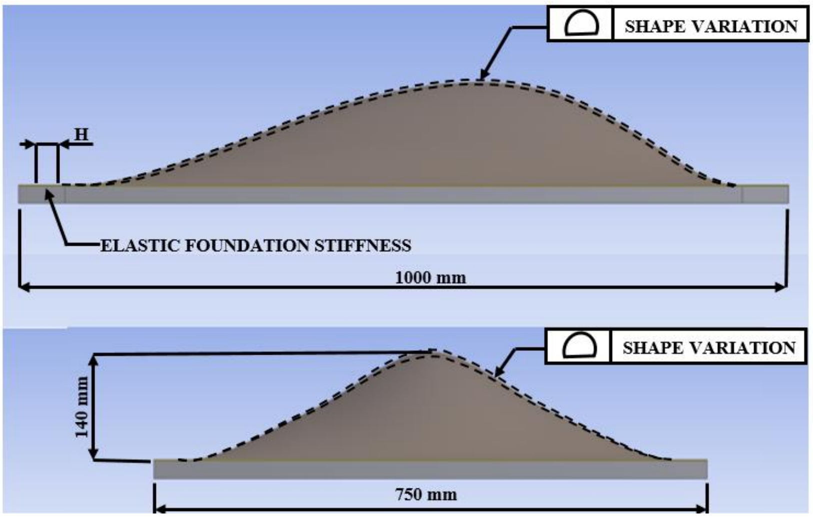

Figure 1 - Shell structure with parametric uncertainties for model updating

A parametric FE model was created using Ansys R14.5, with three parameters to enable the model updating. The first parameter selected for the model updating was the all-around contact surface area between the attached frame and the ATSS, represented by the dimension *H* in Fig.1. This parameter was selected because the ATSS is not precisely located in the frame, and consequently uncertainties are introduced. The second parameter selected was the frame stiffness. In this case, this parameter was selected because the frame does not possess infinite stiffness in the clamping. An elastic foundation was modeled in the contact region between the frame and the ATSS in the all-around contact area defined previously by the first parameter H. The elements created provide a parametric elastic constraint in the translational and rotation degrees of freedom. Finally, the third parameter selected was the shell shape variation. The variation of the shell shape arises from the variability of the stamping process and spring back effects. This variation is known in the industry as shape tolerance and regulated by an ASME standard (ASME, Y14.5-2009). For the implementation of the shape variation parameter, according with Fig. 1, an APDL language routine was created. With these three parameters selected, the model updating was performed using the ranges defined in Tab.1, taken the results obtained in the experimental modal analysis as reference, according with Fig. 2(b).

Table 1- Model updating final parameters (deterministic)

Model Updating				
Objective Function		Freq. (Hz)	192 Hz (reference)	
Parameters				Result
Name	Nominal	Range	Value	
H Frame	*35 mm*	*Min.*	*34 mm*	***34,08 mm***
		Max.	*36 mm*	
Elastic Found. Stiffness	*1,0 x 10^5 N/mm^2*	*Min.*	*9,0 x 10^4 N/mm^2*	***9,78 x 10^4 N/mm^2***
		Max.	*1,1 x 10^5 N/mm^2*	
Shape Var. (Shell)	*Nominal*	*Min.*	*-2,50%*	***1,10%***
		Max.	*2,50%*	

The experimental modal analysis was performed using the GEOMETRY SCAN UNIT (Polytec PSV-A-420) presented in Fig. 2(a). The analysis had employed 320 measurement points in the ATSS using the SCANNER UNIT to define the mode shape and the mechanical resonant frequency of interest in the ATSS. Others 72 independent measurement points specifically in the frame were collected to ensure that the mode shape in analysis was arising only from the ATSS. These others measurement points in the frame are presented in Fig. 2(b) by the green line, showing that in the frame the motion is irrelevant. The vibration mode of interest in the analysis had presented a resonant mechanical frequency of 192 Hz. An interactive optimization routine was implemented in Ansys R14.5 using the Screening Method (Hammersley-Shifted Sampling) for the model updating, with the parameters range presented in Tab.1. The FE model updated is presented in Fig. 2(c).

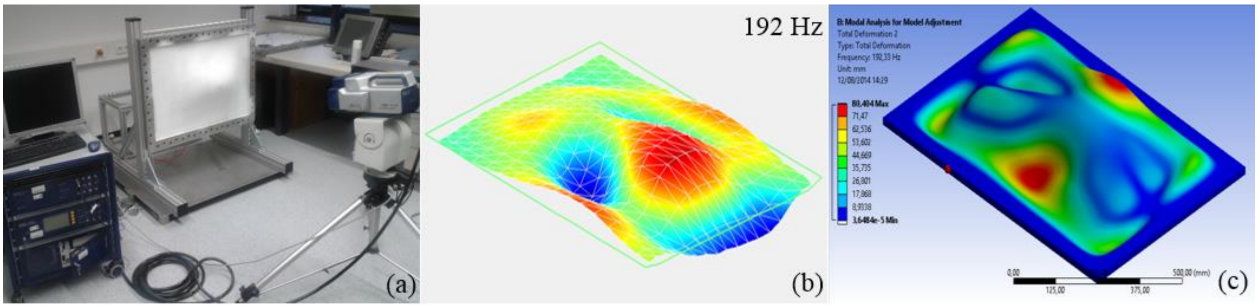

Figure 2 - Experimental modal analysis: (a) apparatus; (b) experimental result; (c) model updated

The three parameters range variation employed in the model updating were defined in possible configuration from the experiment randomness. A preliminary reference for the elastic foundation value was obtained using the screw pressure cone theory from Rötscher in the 60 screws (Shigley and Mischke, 2001). In the present research, the Elasticity Modulus and shell thickness were not considered in the model updating and in the uncertainty quantification. The main reason to consider these parameters deterministic is due the aeronautical and automotive industries use internal undisclosed standards, with very tight tolerances when compared with usual standards. This caution normally is taken to ensure the automatic feeder of stamping machines that uses transfer systems integrating multiple stages of pressing. However, when it is known these specifications, a sensitivity analysis is suggested to understand their impact.

Uncertainties quantification of the arbitrary thin shell structure

After have the FE model updated, the SFEM implementation was conducted to quantify the uncertainties of the dynamic behavior of the ATSS. The primary aspiration to performing the SFEM in the ATSS purely at first was to allow the complete comprehension of the randomness effects in an independent way. The implementation used the Monte Carlo Simulation (MCS) with 5000 samples. A Gaussian distribution for the three parameters susceptible to randomness was employed. The convergence test was conducted previously to ensure that the samples number were enough to ensure the results. The range variation selected for the three parameters were identical to employed previously during the model updating and presented in Tab. 1 (Chen and Koç, 2007) As a result of SFEM, the Probability Density Function (PDF) of the resonant mechanical frequency under uncertainties of the ATSS was obtained and presented in Fig. 3.

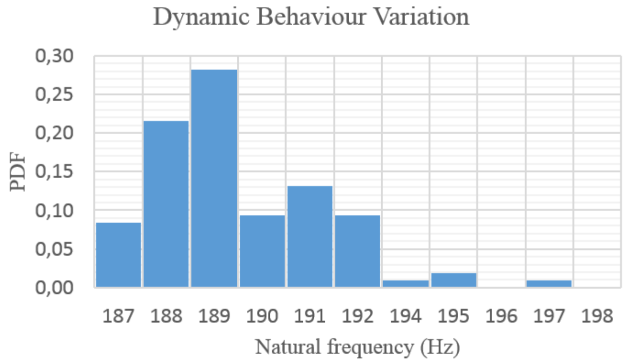

Figure 3 - PDF for ATSS using SFEM

In Fig. 3 could be observed that the effects of the inherent randomness arising from the usual manufacturing process were able to promote one dispersion of approximately 12 Hz in the resonant frequency. One important observation to be held at this point is that for effectiveness of passive shunt damping the correct tuning of the shunt circuits is essential. With dispersion range with this magnitude, the effectiveness of the technique will be impaired. Even with the existence of researches in adaptive shunt circuits, the present research had focus also in quantify the uncertainties of the mechanical resonant frequency, once that the major part of the researches conducted in the adaptive shunt circuits had focus in the PZT capacitance variability due the temperature variation (Moheimani, 2006). In addition, could be observed that the PDF does not present a Gaussian distribution aspect. In order to get a better interpretation of the results, the four statistical moments were winkle out and presented in Tab. 2.

Table 2 - Statistical results

Statistical results	Values
Mean	190,37
Standard deviation	1,83
Kurtosis	1,17
Skewness	1,02

The results presented in Tab. 2 confirms the asymmetry of the FDP and the left side tendency. Aiming to obtain a better understand in the mechanical resonant frequency variability of the ATSS and identify the majors contributor, a sensitivity analysis was conducted and presented in Fig. 4.

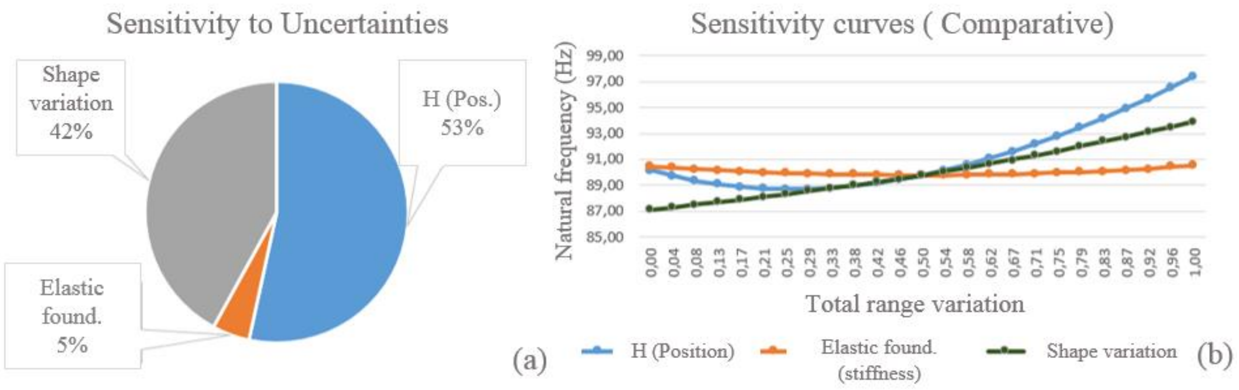

Figure 4 - Sensitivity Analysis for ATSS using SFEM

In Fig. 4, item (a) presents the weights of the uncertain parameters in the SFEM model in percentage term; item (b) represents the comparative sensitivity analysis between the uncertain parameters. Looking for items (a) and (b) jointly, becomes clear that the Elastic Foundation Stiffness variation possesses a very low impact weight in the ATSS dynamical behavior. For the case of the frame interface area and shape variations, the impact weights in the ATSS dynamical behavior are very similar, however with different sensitivity characteristics according with item (b). The shape variation of the ATSS possesses linear sensitivity because when its increase, the ATSS global stiffness also increase. For the frame interface variation area a parabolic sensitivity curve was obtained, once that the ATSS is centralized in the frame.

Piezoelectric optimization under uncertainties

Piezoelectric transducers convert mechanical energy, normally arising from the displacement of mechanical vibrations, into electrical energy. Thereby shunt damping technique could use this electrical energy to neutralize resonant modes or dissipate energy from the mechanical structure (Neubauer and Wallaschek, 2013). For that, the piezoelectric patch needs to have an optimized configuration, in its dimensions and positioning (Ducarne; Thomas; Dëu, 2012; Bachmann; Bergamini; Ermanni, 2012). In the same way, be insensitive to the inherent randomness of the entire system. The effectiveness is measured, weighted and analyzed based on the EMCC defined from Equation (11), which needs to be maximized and insensible to randomness.

The present research had used an innovative procedure to solve the major problem normally found in the EMCC optimization in asymmetric shell structures. An interactive routine able to accomplish the changes in the piezoelectric patches shape curvatures form in each new positioning on the ATSS surface was developed. Likewise, for all new piezoelectric patches dimensions. Putting in others words, during the EMCC optimization routine, the piezoelectric patch was able to travel over the asymmetric shell surface and shaping up to each new configuration. Basically, this routine had created one superior auxiliary parallel plane to the ATSS in each new piezoelectric patch configuration. In this auxiliary plane, the piezoelectric patch possess its original dimensions and posteriorly been projected on the ATSS, representing the attachment application. The entire routine had been created in a parametric way enabling the optimization routine. The details are presented in Fig. 5 (a) and (b).

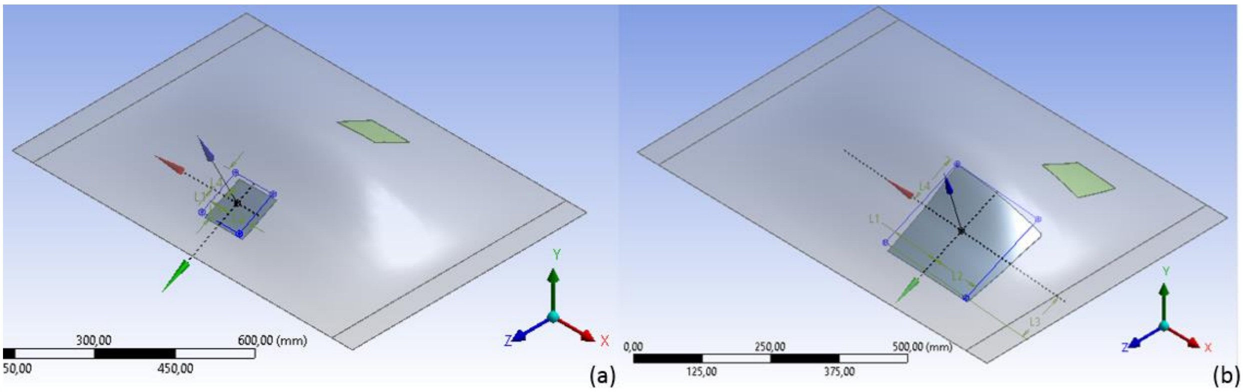

Figure 5 - Piezoelectric patches optimization routine in ATSS surface

For the piezoelectric patch implementation, the solid226 element in ANSYS was employed, together with the PIC 255 piezoelectric material properties, using the ANSYS Parametric Design Language (APDL) (ANSYS and PI-Piezotechnology). The implementation was performed merging the elements nodes to attach the piezoelectric patches in the ATSS surface, according with Fig. 6 (a) in the connection region. For that, the connection between the nodes of the meshes were reconfigured in each new configuration and positioning of the piezoelectric patch. Distinct boundary conditions for the piezoelectric patches were created using APDL language, connection the upper and the lower elements surface, aiming to represent the piezoelectric patch electrodes. After that, two modal analysis were performed using the open and closed electrodes configuration, serving for the calculation of EMCC during the optimization routine, according with Equation (11).

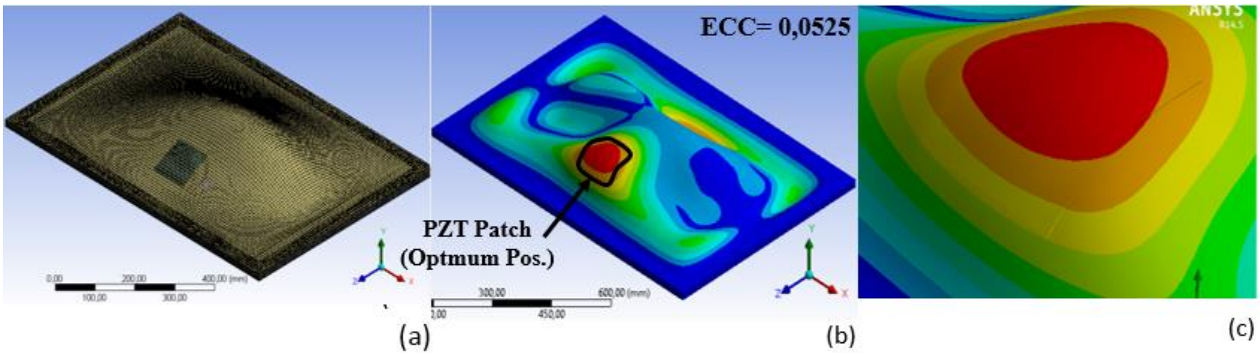

Figure 6 - PZT patches optimized in ATSS surface

The MOGA (Multi Objective Genetic Algorithm) routine was implemented to optimize with high importance the EMCC and in the same time minimize the piezoelectric patch dimensions with lower importance. The minimization of the piezoelectric patch dimensions had also taken into considerations once that the implementation cost and the mass reduction are also important for the project objectives. The optimal configuration is presented in Figure 6(b) and (c), given an EMCC of 0,0525. The optimization routine was able to position the piezoelectric patch in any place of the ATSS surface, with restriction in 100 mm maximum for the width and length dimensions and thickness range between 0,3mm to 0,8 mm.

In order to support subsequent analysis, in the selection of the appropriated flexible piezoelectric patch available in the market, a sensitivity analysis was performed and presented in Fig. (7). In the Fig. 7(a) is presented the EMCC sensitivity with the PZT patch thickness variation; item (b) is presented EMCC sensitivity with the PZT patch width and length dimensions variation; item (c) is presented EMCC sensitivity with the X position variation; and item (d) is presented EMCC sensitivity with the Z position variation.

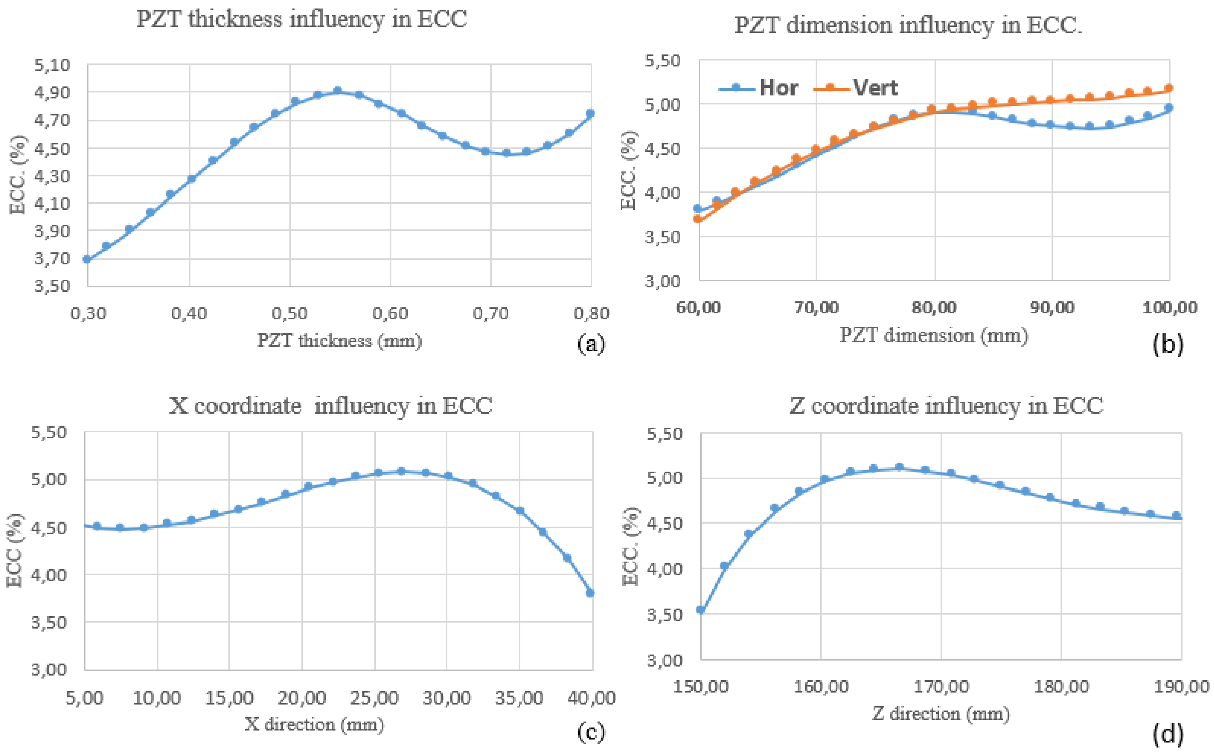

Figure 7 - Sensitivity analysis for the piezoelectric optimization

Looking in the Fig. 7(a), could be observe that for very thick PZT the effectiveness will decrease due to its stiffness. In this way, the thickness configuration that maximizes the EMCC is around 0,5 mm to 0,6 mm. Now using the Figure 7(b) is clear that the biggest patch maximize the EMCC, since that there is no inflection point in the mode of interest. Consequently, the maximum constrain configuration of 100 mm in width and length dimensions is a good option. These analysis had directed to select the flexible PZT patch available in the market and presented in Tab. 3. Its representation could be seen in Fig. 6 providing an EMCC of 5,25%.

Table 3 - Optimized PZT patch specification

Model	Dimension [mm]	Mass [g]	Area [cm^2]
P-876.B42	100 x 100 x 0,5	20	100

Once that the optimal patch was selected, the uncertainties need to be quantified using SFEM. For a robust implement of PZT patch in ATSS, the EMCC needs to be not highly susceptive to uncertainties arising from the whole system randomness, in order to maintain its effectiveness, as mentioned previously. Due the low randomness of the piezoelectric patch width, length and thickness dimensions arising from the fabrication process, these parameters will be considered as deterministic in the SFEM analysis. Similarly, the variation from the shell shape and frame interface area, which are important just for the uncertainties in the mechanical resonant frequency variation of the ATSS and presenting a very low impact in EMCC variation only. In this way the important parameter that really have impact in the EMCC variation is the patch positioning, for this typical application in ATSS and using piezoelectric patch available in the market.

The SFEM implementation used MCS with 5000 samples considers the variation of the positioning as Gaussian distributed parameters with range of ± 2 mm in X and Z coordinates in the ATSS. The Y coordinate is implicit, according with Figure 6. This range was selected, considering the typical precise positioning process capability of automotive and aeronautical industries [16].The SFEM results for quantify the uncertainties in the EMCC are presented in the Fig. 8. In Fig.8 (a), is presented the PDF of the EMCC with X coordinate variation; item (b) is presented the PDF of the EMCC with Z coordinate variation; item (c) is presented the PDF of the EMCC with X and Z coordinates variation together and item (d) is presented the weights of the uncertain parameters in the model in percentage terms.

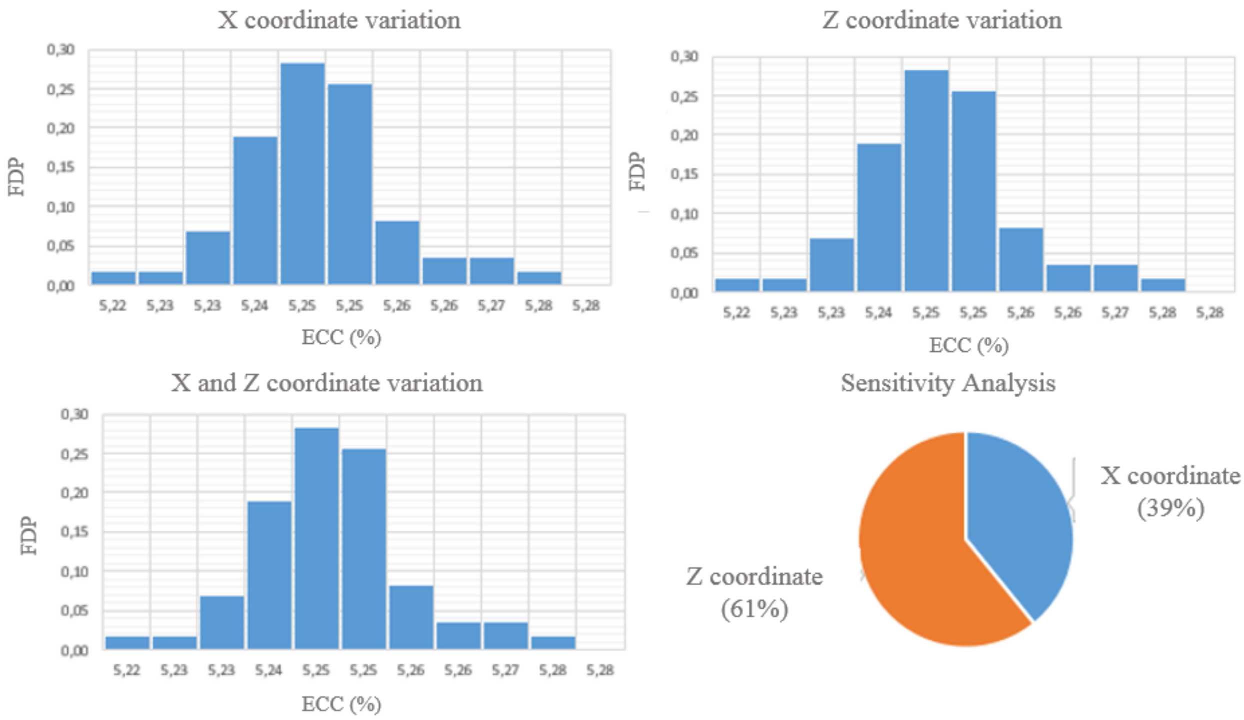

Figure 8 - Uncertainties quantification for PZT positioning (EMCC)

According with Fig. 8, the effects of PZT patch positioning variation possesses low impact in the EMCC, when precise positioning processes are applied. However, connecting Fig. 8 and Fig. 7(c) and (d), is clear that the EMCC is high sensible for positioning variation and strict range tolerances needs to be employed in order to ensure the piezoelectric implementation effectiveness for vibration suppression. Thus, can be observed that for the implementation in large scale production, a serious attention need to be addressed in the manufacture process capability to ensure the correct positioning of the piezoelectric patch.

CONCLUSIONS AND REMARKS

The present research had demonstrated that a systematic approach using SFEM to quantify the uncertainties in the optimal piezoelectric implementation in ATSS is extremely convenient. The results obtained had demonstrated that the inherent randomness of the ATSS resulted in a large spectral range for the dynamic behavior of the mechanical structure. Could be concluded that using conventional manufacture process tolerance values, the range variation of 12 Hz was obtained, with a non-Gaussian distribution. Since for the shunt damping technique effectiveness the correct tuning is essential, this large spectral range need to be analyzed together with the proposed shunt circuit. One important contribution from this paper is to quantify the uncertainties in the mechanical behavior, once that adaptive shunt circuits normally take into the account the piezoelectric capacitance variability only. In this way, a new approach need to be intended to specify the range for adaptive shunt circuits, involving uncertainties from electrical circuits and complex mechanical structures of interest using SFEM.

The SFEM associated with sensitivity analysis had demonstrated to be extremely convenient to quantify the uncertainties in the optimal piezoelectric patch and in the resonant mechanical frequency, serving to guide scientists and engineers to implement shunt damping in real applications. The sensitivity analysis could support engineers and scientists in decision making in order to reduce the dynamical behavior spectrum range using inverse analysis integrated with manufacture process capability. Another important observation is that the piezoelectric patch positioning is paramount to maximize the EMCC in the eigenform of interest. In the same way, a precise positioning tolerance is needed in order to not influence in the effectiveness of the EMCC. Finally, with the support of sensitivity analysis in the piezoelectric optimization, could be observed that for very thick piezoelectric patches the EMCC will decrease due to its stiffness. In this way an optimum PZT thickness is required. For the present research the thickness between 0,5 mm and 0,6 mm maximizes the EMCC.

ACKNOWLEDGMENTS

The authors acknowledge the MCT/CNPq/FAPEMIG National Institute of Science and Technology on Smart Structures in Engineering, grant nr. 574001/2008-5, the CAPES, grant PROBRAL nr. 385-11 and the German federal State of Hessen, project "LOEWE Zentrum AdRIA: Adaptronik - Research, Innovation, Application", grant III L 4 - 518/14004(2008)) for their financial support. The authors thank Tobias Melz, Luiz C.S. Góes, Oliver Heuss, Torsten Bartel, Mihail Lilov and Jorge A.B. Gripp for their support during this research.

REFERENCES

Vanderplaatz, G.: "Numerical optimization techniques for engineering design" Vanderplaatz Research & Development, Fourth Edition, 2005.

Scinocca, F.: Master Thesis "Uncertainty quantification of aircraft modal analysis using perturbation technique in the stochastic finite element method", ITA, Brazil, 2012.

Martowicz, A.; Tadeusz, U.; "Reliability- and performance-based robust design optimization of MEMS structures considering technological uncertainties", Mechanical Systems and Signal Processing, Uncertainties in Structural Dynamics, Vol.32, pp. 44 – 58, 2012;

Ghanem, R.G.; Spanos, P.D.: "Stochastic Finite Elements – A Spectral Approach", Dover Publications, New York, USA, 2003.

Soize, C.: "Stochastic modeling of uncertainties in computational structural dynamics—Recent theoretical advances", Journal of sound and vibration, Vol. 332, pp.2379-2395, 2013;

Stefanou, G.: "The stochastic finite element method: Past, present and future ", Computational Methods Applied in Mechanical Engineering, Vol.198, pp. 1031–1051, 2009.

McKenna, R.; et.al. : "Energy savings through direct secondary reuse: an exemplary analysis of the German automotive sector", Journal of Cleaner Production, Vol. 52, pp. 103 – 112, 2013.

Cirak, F.; et.al. : "Integrated modeling, finite-element analysis, and engineering design for thin-shell structures using subdivision", Computer-Aided Design, Vol. 34, pp. 137 – 148, 2002.

Zhang, Y.; Zhu, P.; Chen, G.: "Lightweight Design of Automotive Front Side Rail Based on Robust Optimization", Thin-Walled Structures, Vol. 45, pp. 670 – 676, 2007.

Maresa, C.; Mottersheadb, J.E.; Friswell, M.I.: " Stochastic model updating: Part 1- theory and simulated example", Mechanical Systems and Signal Processing, pp 1674 – 1695, 2006.

J.E. Mottershead, J.E., et al.: "Stochastic model updating: Part 2—application to a set of physical structures", Mechanical Systems and Signal Processing, Vol. 20, pp. 2171 – 2185, 2006.

John E. Mottershead, J. E.; Link, M.; Friswell, M.I.: "The sensitivity method in finite element model updating: A tutorial", Mechanical Systems and Signal Processing, Vol. 25, pp.2275-2296, 2011.

ASME Y14.5-2009 : "Geometric Dimensioning and Tolerancing", American Society of Mechanical Engineers, 2009.

Shigley, J.E.; Mischke, C.R.: "Mechanical engineering design", McGraw-Hill Series in Mechanical Engineering, 1248pp, 2001.

Chen, P.; Koç, M.: "Simulation of spring-back variation in forming of advanced high strength steels", Journal of Materials Processing Technology, Vol. 190, pp.189–198, 2007.

Moheimani, S.O.R.; Fleming, A.J.: " Piezoelectric Transducers for Vibration Control and Damping", Spring-Verlag, Londom Limited, 2006.

Ducarne, J; Thomas, O.; Dëu, J.-F.: "Placement and dimension optimization of shunted piezoelectric patches for vibration reduction", Journal of Sound and Vibration, Vol. 331, pp-3286 – 3303, 2012.

Bachmann, F.; Bergamini, A.E.; Ermanni, P.: "Optimum piezoelectric patch positioning: A strain energy-based finite element approach", Journal of Intelligent Material Systems and Structures, Vol. 23(14), pp. 1575–1591, 2012

ANSYS, Inc. Theory Reference [online], http://www1.ansys.com/customer/content/documentation/

PI-Piezotechnology (www.piezoceramic.de)

RESPONSIBILITY NOTICE